

Expectile Periodograms

Tianbo Chen¹

Abstract

In this paper, we introduce a periodogram-like function, called expectile periodograms, for detecting and estimating hidden periodicity from observations with asymmetrically distributed noise. The expectile periodograms are constructed from trigonometric expectile regression where a specially designed objective function is used to substitute the squared l_2 norm that leads to the ordinary periodograms. The expectile periodograms have properties which are analogous to quantile periodograms, which provide a broader view of the time series by examining different expectile levels, but are much faster to calculate. The asymptotic properties are discussed and simulations show its efficiency and robustness in the presence of hidden periodicities with asymmetric or heavy-tailed noise. Finally, we leverage the inherent two-dimensional characteristics of the expectile periodograms and train a deep-learning (DL) model to classify the earthquake waveform data. Remarkably, our approach achieves heightened classification testing accuracy when juxtaposed with alternative periodogram-based methodologies.

Keywords: Periodogram; Expectile regression; Spectral density; Time series analysis

1. Introduction

Spectral density functions (SDFs) constitutes a pivotal element within the realm of time series analysis, where the data are analyzed in the frequency domain. Periodograms, a recognized non-parametric estimator of the SDF, are

¹Anhui University, China. E-mail:

widely used in many applications. A notable instance of its deployment resides in Electroencephalogram (EEG) data analysis, where the spectral features revealed by the periodograms are used for disease diagnosis (Polat and Güneş, 2007; Baud et al., 2018; Martínez-Murcia et al., 2019). Furthermore, periodograms find utility in EEG channel clustering Euán et al. (2018); Maadooliat et al. (2018); Chen et al. (2021a). Ordinary periodogram are construed by the ordinary least squares (OLS) regression on the trigonometric regressor, a methodology primarily focuses on the conditional mean. Consequently, the ordinary periodograms may exhibit limitations in terms of robustness and effectiveness, particularly in handling data with asymmetric or heavy-tailed distributions (Bloomfield, 2004).

An alternative regression approach is quantile regression where regression effects on the conditional quantile function of the response are assumed. The pioneering work of Koenker and Bassett Jr (1978) introduced the concept of quantile regression, which measures the variation of the conditional quantiles with respect to the response variable. This methodology has been comprehensively extended by Koenker (2005). For a detailed and systematic introduction to quantile regression and some interesting extensions of basic quantile-based models, we refer to Kouretas et al. (2005); Cai and Xu (2008); Cai and Xiao (2012); Koenker (2017). Armed with a specially designed loss function, quantile regression gives a more complete picture of the relationship between the response variable and the covariates, and shows strong robustness against outliers. Quantile regression techniques and their derivatives have been using by researchers all over the fields of science (Garcia et al., 2001; Machado and Mata, 2005; Alvarado et al., 2021; Sharif et al., 2021).

An innovative development in this domain are the quantile periodograms (Li, 2012b), which are constructed by trigonometric quantile regression and show their ability in detecting hidden periodicities in time series. Similarly to the behavior of the ordinary SDFs and periodograms, the quantile periodograms are unbiased estimators of the so-called quantile spectrum, which are scaled version of the ordinary SDFs of the level-crossing process. It is noteworthy that the Laplace periodograms (Li, 2008) represent a specialized case of the quantile

periodograms, specifically when the quantile is set to 0.5. Related works of the quantile periodograms include Li (2012a); Hagemann (2013); Li (2014); Dette et al. (2015); Kley (2016); Birr et al. (2017); Meziani et al. (2020); Chen et al. (2021b); Li (2023).

However, quantile regression is beset by several limitations. Firstly, it entails a heightened computational burden due to the non-differentiability of the loss function. Secondly, quantile regression is less effective for light-tailed noise. Thirdly, the uniqueness of the solution is not guaranteed. In order to balance robustness and effectiveness To address these shortcomings, the concept of expectile regression has been introduced. The asymmetric least square (ASL) regression, known as expectile regression, was proposed in Newey and Powell (1987). While quantile regression can be regarded as a generalization of median regression, expectile regression can be seen as a combination of the OLS regression and quantile regression. Expectile regression exhibits the ability of measuring the whole distribution of the data and is much easier to compute using quadratic optimization. A comprehensive comparative analysis of quantiles and expectiles is presented in Waltrup et al. (2015), wherein the relationships between these two approaches are thoroughly examined. Jones (1994) provides mathematical proof that expectiles indeed correspond to quantiles of a distribution function uniquely associated with the underlying data distribution. Furthermore, Yao and Tong (1996) establish the existence of a unique bijective function mapping expectiles to quantiles, thereby facilitating the calculation of one from the other. Alternative approaches for estimating quantiles from expectiles are introduced in Efron (1991); Granger and Sin (1997); Schnabel and PHC (2009), elucidating methodologies for estimating the density (and also, quantiles) from a set of expectiles by using penalized least squares. As an generalization of quantile regression and expectile regression, Jiang et al. (2021) introduce the k -th power expectile regression with $1 < k \leq 2$.

Expectile regression techniques have found applicability across diverse domains. Jiang et al. (2017) introduces an expectile regression neural network (ERNN) model. This novel approach incorporates a neural network structure

into expectile regression, thereby facilitating the exploration of potential nonlinear relationships between covariates and the expectiles of the response variable. Gu and Zou (2016) systematically study the Sparse Asymmetric Least Squares (SALES) regression under high dimensions where the penalty functions include the Lasso and nonconvex penalties. Xu et al. (2020) develops a novel mixed data sampling expectile regression (MIDAS-ER) model to measure financial risk and demonstrated exceptional performance when applied to two popular financial risk measures: Value at Risk (VaR) and Expected Shortfall (ES). Xu et al. (2021) have introduced the elastic-net penalty into expectile regression, and applied the model to two real-world applications: relative location of CT slices on the axial axis and metabolism of tacrolimus drug.

In response to the notable accomplishments achieved through expectile regression and the conceptual foundation of the quantile periodograms, we employ expectile regression to define a novel spectral estimator termed the expectile periodograms, for spectral analysis of time series data. In this paper, we demonstrate that the expectile periodograms not only share similar properties of the ordinary periodograms as a frequency-domain representation of the serial dependence within the time series, but also provide a richer source of information in comparison to the ordinary periodograms. The paper is organized as follows. In section 2, we define the expectile periodograms and make a comparison to the ordinary and quantile periodograms. In Section 3, we present comparative studies on the performances of the different periodograms on simulated data. In Section 4, we apply our method to a time-series classification task. We take advantage of the two-dimensional property of the expectile periodograms and train a deep-learning (DL) model to classify the earthquake data. The conclusion and future work are discussed in Section 5.

2. Expectile Periodograms

In this section, we define the expectile periodograms and make comparisons to the ordinary and the quantile periodograms.

Given an expectile level $\tau \in (0, 1)$, define the ALS (Newey and Powell, 1987) cost function of the form

$$\rho_\tau(u) = |\tau - I(u < 0)| \cdot u^2,$$

where $I(\cdot)$ denoting the indicator function. For a time series $\mathbf{Y} = \{Y_1, Y_2, \dots, Y_n\}$, the sample τ -expectile $\hat{\lambda}_n$ minimizes the cost function:

$$\hat{\lambda}_\tau = \arg \min_{\lambda \in \mathbb{R}} \sum_{t=1}^n \rho_\tau(Y_t - \lambda)$$

Consider the linear trigonometric expectile regression solution

$$\hat{\boldsymbol{\beta}}_{n,\tau}(\omega) := \arg \min_{\boldsymbol{\beta} \in \mathbb{R}^2, \lambda_\tau \in \mathbb{R}} \sum_{t=1}^n \rho_\tau\{Y_t - \lambda_\tau - \mathbf{x}_t^\top(\omega)\boldsymbol{\beta}(\omega)\}, \quad (1)$$

where $\mathbf{x}_t(\omega) = \{\cos(\omega t), \sin(\omega t)\}^\top$ is the trigonometric regressor for the propose of detecting the hidden periodicity with $\omega \in (0, \pi)$, λ_τ is a suitable constant, typically the τ -expectile of \mathbf{Y} , and $\boldsymbol{\beta}(\omega) = [\beta_1(\omega), \beta_2(\omega)]$. Aigner et al. (1976) showed that the estimator can be interpreted as a maximum likelihood estimator when the disturbances arise from a normal distribution with unequal weight placed on positive and negative disturbances. Then, we define the expectile periodograms at expectile level τ as

$$EP_{n,\tau}(\omega) := \frac{1}{4}n\|\hat{\boldsymbol{\beta}}_{n,\tau}(\omega)\|_2^2 = \frac{1}{4}n\hat{\boldsymbol{\beta}}_{n,\tau}^\top(\omega)\hat{\boldsymbol{\beta}}_{n,\tau}(\omega).$$

The expectile periodogram measure the total power of the trigonometric regressor. The parameter λ_τ is fixed in (1), it can also be optimized with $\boldsymbol{\beta}(\omega)$ to obtain the extended expectile regression solution

$$\{\hat{\lambda}(\omega), \hat{\boldsymbol{\beta}}_{n,\tau}(\omega)\} := \arg \min_{\boldsymbol{\beta} \in \mathbb{R}^2, \lambda_\tau \in \mathbb{R}} \sum_{t=1}^n \rho_\tau\{Y_t - \lambda_\tau - \mathbf{x}_t^\top(\omega)\boldsymbol{\beta}(\omega)\}$$

The expectile periodograms can be regarded as extensions of the ordinary periodograms and quantile periodograms. For ordinary periodogram $I_n(\omega) := \frac{1}{n} \left| \sum_{t=1}^n Y_t e^{-2\pi j t \omega} \right|^2$, it is easy to verify that when ω is a Fourier frequency of the form $2\pi l/n$ ($l \in \mathbb{Z}^+$), we can write

$$I_n(\omega) := \frac{1}{4}n\|\bar{\boldsymbol{\beta}}_n(\omega)\|_2^2, \quad (2)$$

where $\bar{\beta}_n(\omega)$ is given by the OLS

$$\bar{\beta}_n(\omega) := \arg \min_{\beta \in \mathbb{R}^2, \mu \in \mathbb{R}} \sum_{t=1}^n \{Y_t - \mu - \mathbf{x}_t^\top(\omega)\beta(\omega)\}^2,$$

and μ is the sample mean. The ordinary periodograms are constructed by least squares techniques, which focus on the conditional mean of the response variable given the predictors. Conversely, the quantile periodograms are constructed through the utilization of quantile regression methods, offering a more comprehensive perspective of the data by exploring various quantile levels. Furthermore, quantile regression exhibits robustness in the presence of asymmetrically distributed noise and nonlinear distortions. Substituting the OLS regression with quantile regression, we have

$$\tilde{\beta}_{n,\alpha}(\omega) := \arg \min_{\beta \in \mathbb{R}^2, \lambda_{t\alpha} \in \mathbb{R}} \sum_{t=1}^n \rho_\alpha^* \{Y_t - \lambda_{t\alpha} - \mathbf{x}_t^\top(\omega)\beta(\omega)\},$$

where $\rho_\alpha^*(u) = u\{\alpha - I(u < 0)\}$, the quantile periodograms at quantile level $\alpha \in (0, 1)$ is defined in Li (2012b) as

$$QP_{n,\alpha}(\omega) := \frac{1}{4}n\|\tilde{\beta}_{n,\alpha}(\omega)\|_2^2 = \frac{1}{4}n\tilde{\beta}_{n,\alpha}^\top(\omega)\tilde{\beta}_{n,\alpha}(\omega). \quad (3)$$

With $\alpha = 0.5$, the quantile periodograms reduce to the Laplace periodogram proposed in Li (2008).

The expectile periodogram is a versatile analytical tool that can be conceptualized in two distinct aspects. Firstly, it can be viewed as a “curve” corresponding to a specific expectile level. Secondly, it can be examined as a bivariate “surface” or “image” defined over the parameters τ and ω . This dual perspective augments our capacity to glean deeper insights into the temporal characteristics of time series data. In Figure 1, we demonstrate the capabilities inherent to the expectile periodograms in detecting hidden periodic patterns within a GARCH(1,1) (Bollerslev, 1986) process: $Y_t \sim N(0, \sigma_t^2)$, $\sigma_t^2 = 10^{-6} + 0.35Y_{t-1}^2 + 0.35\sigma_{t-1}^2$ ($t = 1, \dots, 200$). Figure 1 (a) portrays the averaged expectile periodograms obtained from 5,000 Monte Carlo simulation runs. Notably, the expectile periodograms successfully identify low-frequency spectral

power at both the lower and upper expectiles. In contrast, the ordinary periodograms yield a relatively featureless flat line (similar to the performance of the expectile periodograms near $\tau = 0.5$).

The principal of this paper is analyzing the serial dependence of the time series, with amplitude considerations being of secondary importance. So we normalize all types of periodograms: the summation over ω equals to unity.

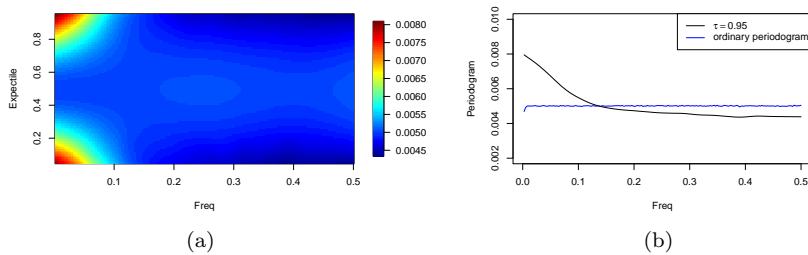


Figure 1: (a) The averaged expectile periodograms of a GARCH(1,1) model; (b) the comparison of the expectile periodogram at $\tau = 0.95$ and the ordinary periodogram.

3. Numerical Results

In this section, we show some numerical results to demonstrate the efficiency of the expectile periodograms, which is a powerful tool in detecting hidden periodicities in time series. We use the following model:

$$Y_t = a_t X_t, \quad (4)$$

$$a_t = b_0 + b_1 \cos(\omega_0 t) + b_2 \sin(\omega_1 t),$$

with $(b_0 = 1, b_1 = 0.9, b_2 = 1)$ and $\{X_t\}$ is an AR(2) process satisfying

$$X_t = \phi_1 X_{t-1} + \phi_2 X_{t-2} + \epsilon_t, \quad (5)$$

with $\phi_1 = 2r \cos(\omega_c), \phi_2 = -r^2$ ($r = 0.6$) and $\{\epsilon_t\}$ is the noise. Additionally, we set $\omega_0 = 0.1 \times 2\pi, \omega_1 = 0.12 \times 2\pi$, and the parameter λ_τ is taken to be the sample τ -expectile of the time series. The purpose is to test the eligibility of different types of periodograms in detecting multiple close periodicities.

Like the ordinary periodogram and the quantile periodogram, the expectile periodogram can serve as representations of serial dependence in the frequency of the time series with no hidden periodicities. We first present the periodograms defined by (5) with $\omega_c = 0.25$ and 0.3 . As shown in Figure 2, the ordinary and the smoothed expectile periodogram exhibit a similar bell-shaped pattern (with large power around ω_c) expected for the SDF of the AR(2) process (Shumway and Stoffer, 2016). Specifically, Figure 2 shows the ensemble means of 5000 smoothed periodograms (both ordinary and expectile), using `smooth.spline` in R with the tuning parameters selected by generalized cross-validation (GCV).

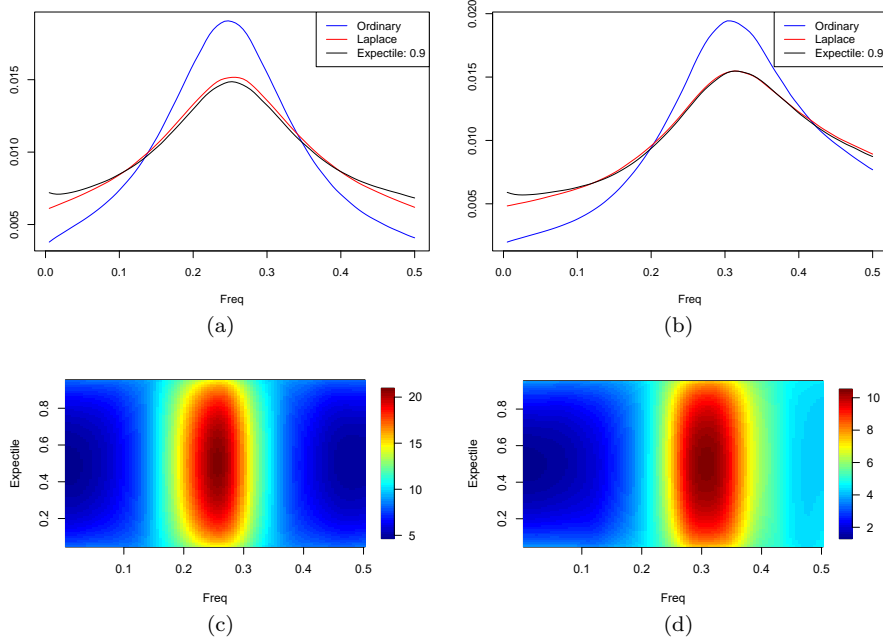


Figure 2: Ensemble mean of three types of smoothed periodograms of time series defined by (5) with standard Gaussian white noise. (a) the ordinary periodogram, (b) the expectile periodograms at $\tau = 0.9$ and (c) the expectile periodograms at $\tau = \{0.05, 0.06, \dots, 0.94, \dots, 0.95\}$. The number of realisations is 5000 and the sample size $n = 200$.

Figure 3 demonstrates the ability of the expectile periodograms in detecting hidden periodicities. We present the mean of 5000 realizations of the ordinary and the expectile periodograms of model 4, the expectile periodograms

detect the hidden periodicities as spikes at ω_0 and ω_1 , whereas the ordinary periodograms fail to do so. We point out that spectral leak, which has been observed for the Laplace periodograms and the quantile periodograms, is also possible for the expectile periodograms. Therefore, small spikes may occur at some other frequencies, as suggested by Theorem 2 in Li (2012b). Adding an l_1 penalty to the regression could be a possible solution to the spectral leakage.

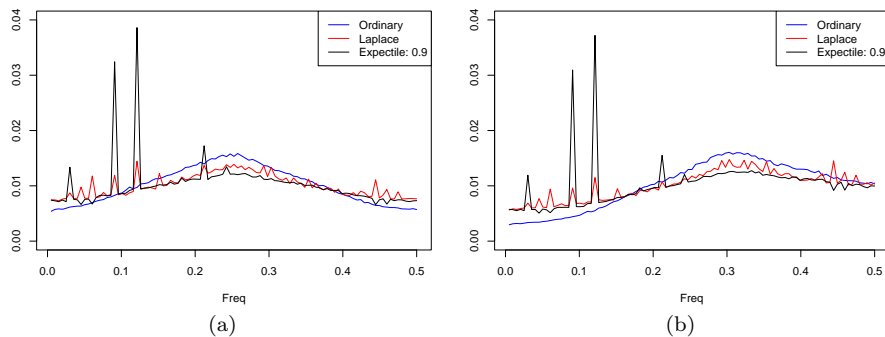


Figure 3: Mean of the three types of periodograms of time series defined by (4). (a) Represents $\omega_c = 0.25$ and (b) with $\omega = 0.3$. The number of realisations is 5000 and the sample size $n = 200$.

The expectile periodograms demonstrated in Figure 1 and 2 are symmetric across the expectile level. We constructed Y_t , a nonlinear mixture of three components, which is defined by:

$$\begin{aligned}
 Z_t &= W_1(X_{t1}) X_{t1} + \{1 - W_1(X_{t1})\} X_{t2}, \\
 Y_t &= W_2(Z_t) Z_t + \{1 - W_2(Z_t)\} X_{t3}. \tag{6}
 \end{aligned}$$

The components $\{X_{t1}\}$, $\{X_{t2}\}$, and $\{X_{t3}\}$ are independent Gaussian AR(1) processes satisfying

$$\begin{aligned}
 X_{t1} &= 0.8X_{t-1,1} + w_{t1}, \\
 X_{t2} &= -0.75X_{t-1,2} + w_{t2}, \\
 X_{t3} &= -0.81X_{t-2,3} + w_{t3},
 \end{aligned}$$

where w_{t1}, w_{t2}, w_{t3} are standard Gaussian white noise. From the perspective of traditional spectral analysis, the series $\{X_{t1}\}$ has a lowpass spectrum, $\{X_{t2}\}$ has a highpass spectrum, and $\{X_{t3}\}$ has a bandpass spectrum around frequency $1/4$. The mixing function $W_1(x)$ is equal to 0.9 for $x < -0.8$, 0.25 for $x > 0.8$, and linear transition for x in between. The mixing function $W_2(x)$ is similarly defined except that it equals 0.5 for $x < -0.4$ and 1 for $x > 0$. Figure 4 shows the expectile periodograms of (6), where the expectile periodogram is asymmetric across the expectile level.

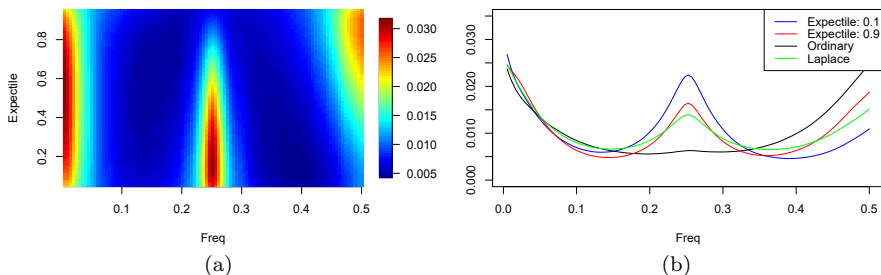


Figure 4: The periodograms of the mixture model defined by (6). (a) The expectile periodogram with asymmetric pattern across the expectile level, and (b) the expectile periodograms at extreme expectiles ($\tau = 0.1$ and 0.9), as well as the ordinary and the Laplace periodograms. The number of realisations is 5000 and the sample size $n = 200$

Based on the ordinary periodogram, one commonly used hypothesis test for detecting periodicity of time series is Fisher's test (Brockwell and Davis, 1991). For $\omega = \{\omega_1, \omega_2, \dots, \omega_l\}$, the test statistic is defined by

$$g = \frac{\max_{1 \leq k \leq l} \{I_n(\omega_k)\}}{\sum_{k=1}^l I_n(\omega_k)}. \quad (7)$$

Fisher's test implies the presence of hidden periodicity if g is sufficiently large. The null hypothesis that the time series is Gaussian white noise against the alternative hypothesis that the time series contains a deterministic periodic component of unspecified frequency. The idea is to reject the null hypothesis if g take a sufficiently large value. We apply the Fisher's test on expectile periodogram by replacing $I_n(\omega)$ with $EP_{n,\tau}(\omega)$. The probabilities of detection is obtained by Monte Carlo simulation runs for time series defined by (4), with

a single periodicity: $\omega_0 = 0.1 \times 2\pi$, $\omega_c = 0.3 \times 2\pi$, and $b_2 = 0$. The results of the test is demonstrated in Table 1. The expectile periodograms and the quantile periodograms outperform than the ordinary periodograms. At significance level 0.05, the expectile periodogram ($\tau = 0.9$) reaches the detection rate 84.26%, whereas the detection rate of the ordinary periodogram is 29.78%. The detection rates depend on the expectile level. In this experiment, as the expectile and quantile close to 1, the detection rate of expectile periodograms has a increasing trend and surpasses the quantile periodograms.

Table 1: Fisher’s test of different types of periodograms

Significa- nce level	Expectile periodograms			Quantile periodograms			Ordianry p- eriodograms
	$\tau=0.85$	$\tau=0.9$	$\tau=0.95$	$\alpha=0.85$	$\alpha=0.9$	$\alpha=0.95$	
0.01	0.4048	0.5608	0.5850	0.6898	0.6328	0.4428	0.1224
0.05	0.7158	0.8426	0.8510	0.8720	0.8260	0.6646	0.2978
0.10	0.8308	0.9262	0.9306	0.9278	0.8952	0.7678	0.4258

4. Earthquake Data Classification

In this section, we apply our estimators to an earthquake classification problem. We describe the earthquake data in Section 4.1 and then illustrate the deep learning model and the classification results in Section 4.2.

4.1. Data Description

The earthquake waveform data (sampling rate is 100 Hz) is collected during February 2014 in Oklahoma State, which is available at <https://www.iris.edu/hq/> and <http://www.ou.edu/ogs.html>. Details about the catalog data are provided in Benz et al. (2015), where the magnitudes and times of the earthquakes are labeled. We select four representative

We extract 2000 nonoverlapping segments of data, each being a time series of length 2000 (equivalent to 20 seconds). The purpose of choosing long

time series is to guarantee that the segments contains the complete earthquake events. Among these time series, 1000 of them contain an earthquake with a magnitude higher than 0.25 and the remaining 1000 time series contain no earthquakes. We smooth the expectile periodograms of the 2000 time series using the semi-parametric method proposed in Chen et al. (2021b), where the smoothness of the two dimensions (expectiles and frequencies) are ensured. In this experiment, we use the lower half of the frequencies ($l = 1, 2, \dots, 500$) and 46 expectiles (0.05, 0.07, ..., 0.93, 0.95). Since we focus on the serial dependence and use the normalized expectile periodograms, the amplitude is not considered, which makes the classifications more challenging. We also consider two competitive periodograms: the ordinary periodograms and the quantile periodograms use the same smoothing technique.

We show three representative segments and the corresponding smoothed expectile periodograms in Figure 5, where Figure 5(a) contains a large earthquake with a magnitude larger than 3; Figure 5(b) contains a somehow small earthquake with a magnitude smaller than 1; Figure 5(c) contains no earthquake. Based on the three segments, we have the following features:

- The smoothed expectile periodogram of the segment with a large earthquake has a large power at the low-frequency band in the high and low expectiles.
- The smoothed expectile periodogram of the segment with a small earthquake has peaks at both low frequency band (in low and high expectiles) and high frequency band (in middle expectiles).
- The smoothed expectile periodogram of the segment with no earthquake only have peaks at a higher frequency band.

4.2. Classification using Deep Learning Model

In this section, we use the three types of smoothed periodogram as the feature by which we classify the segments into those that contain earthquakes

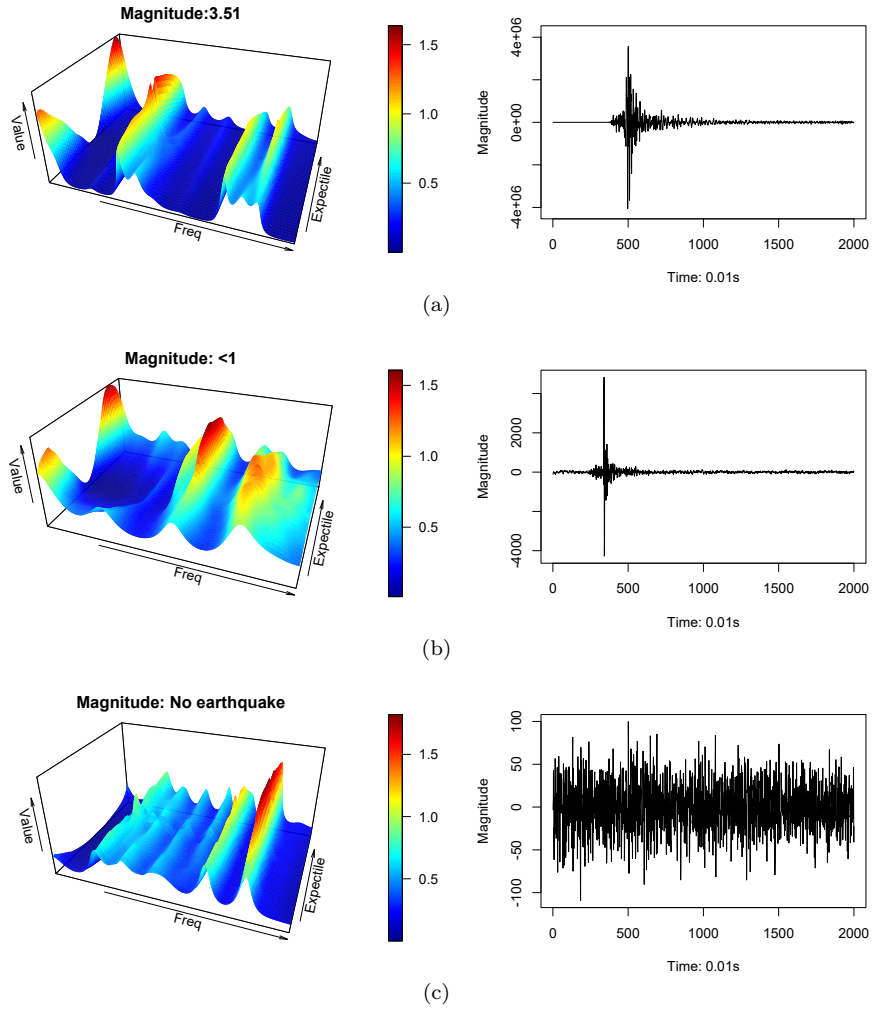


Figure 5: Three segments and the corresponding smoothed expectile periodograms. (a) The segment with an earthquake with a magnitude > 3 , (b) the segment with an earthquake with a magnitude < 1 , and (c) the segment with no earthquake. We use $n = 2000$, $l = 1, 2, \dots, 500$ (half of the frequencies), and $\tau = 0.05, 0.07, \dots, 0.95$ (46 expectiles) in this experiment.

and those that do not. We randomly split the segments into training and testing sets with size 1600 and 400, respectively. To classify the expectile periodograms and the quantile periodograms (2D), we use two convolutional layers to extract the features, each one connected to a maxpooling layers, where the second pooling layer connects to a fully connected (FC) layers after flattened. We

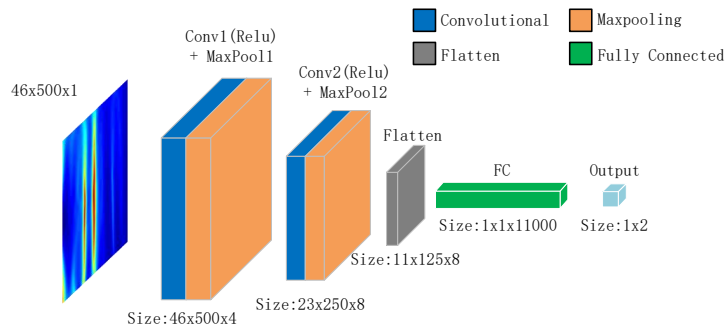


Figure 6: The structure of the deep learning model.

add a dropout layer with a ratio of 50% to the FC, which is connected to the output layer. The total trainable parameters is 2,817,682 and the learning rate is set to be $1e - 4$ with a reduction rate 0.5 every 20 epochs. More details of the model could be found in <https://github.com/tianbochen1>. The structure of the model is shown in Figure 6. To classify the ordinary periodogram (1D), we apply the model shown in Figure 6 with different dimensions of input (46×500 instead of 1×500) and kernel size (5×5 instead of 1×5).

We conduct the training ten times and randomly construct the training-testing split and weights initialization using random seed. Over 80% of the training procedures converge at 30 epochs. The testing accuracy of the three type of periodograms are: expectile periodograms: {0.9900, 1.0000, 0.9925, 1.0000, 0.9975, 0.9950, 0.9925, 0.9925, 0.9950, 0.9925}, quantile periodograms: {0.9825, 0.9900, 0.9925, 0.9925, 0.9825, 0.9950, 0.9925, 0.9900, 0.9875, 0.9825}, and ordinary periodogram: {0.9875, 0.9725, 0.9825, 0.9825, 0.9975, 0.9850, 0.9850, 0.9825, 0.9775, 0.9900}.

The averaged classification results and their standard deviations on testing set are shown in Table 2 and Table 3. The confusion matrices are shown in Table 2, in which true positive (TP) indicates that the segment has an earthquake and is classified as an earthquake; true negative (TN) indicates that the segment has

no earthquake and is classified as no earthquake; false positive (FP) indicates that the segment has no earthquake but is classified as an earthquake; false negative (FN) indicates that the segment has an earthquake but is classified as no earthquake (P: positive, N: negative, T: true and F: false). Table 3 shows three metrics of the classification: accuracy, precision ($\frac{TP}{TP+FP}$), and recall ($\frac{TP}{TP+FN}$). The optimum value in each of the three periodograms in each row is shown in bold.

Table 2: The averaged confusion matrices of the classification.

(a) Expectile odogram	Peri-		(b) Quantile odogram	Peri-		(c) Ordinary odogram	Peri-	
	P	N		P	N		P	N
T	199.3	198.6	T	196.2	199.3	T	196.2	197.5
F	0.7	1.4	F	3.8	0.7	F	3.8	2.5

Table 3: The classification results.

Metrics		Expectile	Quantile	Ordinary
Accuracy	Averaged	0.9948	0.9880	0.9858
	[min, max]	[0.9925, 1.0000]	[0.9725, 0.9950]	[0.9750, 0.9925]
Precision	Averaged	0.9965	0.9840	0.9843
	[min, max]	[0.9896, 1.0000]	[0.9559, 0.9952]	[0.9609, 0.9902]
Recall	Averaged	0.9931	0.9921	0.9877
	[min, max]	[0.9858, 1.0000]	[0.9794, 1.0000]	[0.9653, 1.0000]
Time		0.3739	0.3731	0.1042

From the results, we can see that

- The classification based on expectile periodograms has higher testing accuracy, precision and recall rate than the quantile periodograms and the ordinary periodograms. Specifically, all the testing accuracy in the ten

experiments reach 0.99, and two of them are 1. This indicates that the expectile periodograms are eligible to be the feature in time series classification.

- One misclassification case in FN using expectile periodograms is shown in Figure 7. Since the magnitude is too small (< 0.1), the power at low frequencies is not as large as the power at high frequencies, which causes the misclassification.
- However, the expectile periodograms incur a high computational cost in classification because its dimension is multiplied by the number of expectiles compared to the ordinary periodograms.

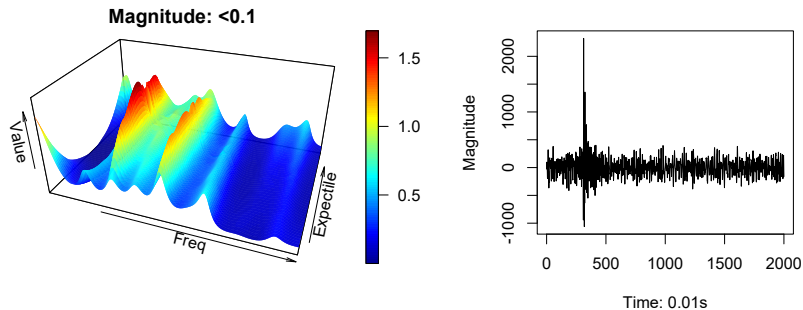


Figure 7: One misclassification case (FN).

5. Conclusion

In this paper, we propose the expectile periodograms, a new frequency domain estimator constructed from trigonometric expectile regression. The expectile periodograms have properties analogous to the quantile periodograms, while distinguished by high computational efficiency. The expectile periodograms offer more information than the ordinary periodogram by examining the serial dependence at different expectile levels. We conduct simulation studies, highlighting their proficiency in detecting hidden periodicities within the time series

data. In the earthquake data classification task, we leverage the inherent two-dimensional characteristics of expectile periodograms using the deep learning model, which is a powerful technique in image classification.

Nevertheless, the expectile periodograms incurs a high computational cost in classification and other applications compared with the ordinary periodograms. This computational burden arises from the fact that the dimensionality of the estimator is multiplied by the number of expectiles employed. As illustrated in Section 4.2, Table 3 reveals a substantial contrast in training times per epoch between the expectile periodograms and ordinary periodograms. Specifically, the training time using expectile periodograms amounts to 0.3739 seconds, while only 0.1042 seconds required when using the ordinary periodograms. These computations were executed on a personal computer equipped with an Intel Core i9-13900KF processor and Nvidia Geforce RTX4090 graphics card. One solution to reduce the computational cost is to use fewer expectiles. In this paper, we choose a large number of expectiles uniformly across $(0, 1)$. Researchers may choose to focus exclusively on a subset of expectiles with sufficient discriminative power (e.g., high or low expectiles). Furthermore, we use multi-thread parallelization to speed up computing using the package `foreach`, `doParallel` in R.

An R code for computing the expectile periodograms and for reproducing the results in Section 3 is accessible at <https://github.com/tianbochen1/>. A Python code of the earthquake earthquake data classification in Section 4 can be found at <https://github.com/tianbochen1/>.

6. Appendix

6.1. *Expectile Regression Theorem*

References

- Aigner, D. J., Amemiya, T., and Poirier, D. J. (1976). On the estimation of production frontiers: maximum likelihood estimation of the parameters of a discontinuous density function. *International economic review*, pages 377–396.
- Alvarado, R., Tillaguango, B., Dagar, V., Ahmad, M., Işık, C., Méndez, P., and Toledo, E. (2021). Ecological footprint, economic complexity and natural resources rents in latin america: empirical evidence using quantile regressions. *Journal of Cleaner Production*, 318:128585.
- Baud, M. O., Kleen, J. K., Mirro, E. A., Andrechak, J. C., King-Stephens, D., Chang, E. F., and Rao, V. R. (2018). Multi-day rhythms modulate seizure risk in epilepsy. *Nature communications*, 9(1):88.
- Benz, H. M., McMahon, N. D., Aster, R. C., McNamara, D. E., and Harris, D. B. (2015). Hundreds of earthquakes per day: The 2014 guthrie, oklahoma, earthquake sequence. *Seismological Research Letters*, 86(5):1318–1325.
- Birr, S., Volgushev, S., Kley, T., Dette, H., and Hallin, M. (2017). Quantile spectral analysis for locally stationary time series. *Journal of the Royal Statistical Society: Series B (Statistical Methodology)*, 79(5):1619–1643.
- Bloomfield, P. (2004). *Fourier analysis of time series: an introduction*. John Wiley & Sons.
- Bollerslev, T. (1986). Generalized autoregressive conditional heteroskedasticity. *Journal of econometrics*, 31(3):307–327.
- Brockwell, P. J. and Davis, R. A. (1991). *Time Series: Theory and Methods*. Springer.
- Cai, Z. and Xiao, Z. (2012). Semiparametric quantile regression estimation in dynamic models with partially varying coefficients. *Journal of Econometrics*, 167(2):413–425.

- Cai, Z. and Xu, X. (2008). Nonparametric quantile estimations for dynamic smooth coefficient models. *Journal of the American Statistical Association*, 103(484):1595–1608.
- Chen, T., Sun, Y., Euan, C., and Ombao, H. (2021a). Clustering brain signals: A robust approach using functional data ranking. *Journal of Classification*, 38:425–442.
- Chen, T., Sun, Y., and Li, T.-H. (2021b). A semi-parametric estimation method for the quantile spectrum with an application to earthquake classification using convolutional neural network. *Computational Statistics & Data Analysis*, 154:107069.
- Dette, H., Hallin, M., Kley, T., Volgushev, S., et al. (2015). Of copulas, quantiles, ranks and spectra: An l_1 -approach to spectral analysis. *Bernoulli*, 21(2):781–831.
- Efron, B. (1991). Regression percentiles using asymmetric squared error loss. *Statistica Sinica*, pages 93–125.
- Euán, C., Ombao, H., and Ortega, J. (2018). The hierarchical spectral merger algorithm: a new time series clustering procedure. *Journal of Classification*, 35:71–99.
- García, J., Hernández, P. J., and Lopez-Nicolas, A. (2001). How wide is the gap? an investigation of gender wage differences using quantile regression. *Empirical economics*, 26:149–167.
- Granger, C. and Sin, C. (1997). Estimating and forecasting quantiles with asymmetric least squares. Technical report, Working Paper, University of California, San Diego.
- Gu, Y. and Zou, H. (2016). High-dimensional generalizations of asymmetric least squares regression and their applications.
- Hagemann, A. (2013). Robust spectral analysis.

- Jiang, C., Jiang, M., Xu, Q., and Huang, X. (2017). Expectile regression neural network model with applications. *Neurocomputing*, 247:73–86.
- Jiang, Y., Lin, F., and Zhou, Y. (2021). The k th power expectile regression. *Annals of the Institute of Statistical Mathematics*, 73:83–113.
- Jones, M. C. (1994). Expectiles and m -quantiles are quantiles. *Statistics & Probability Letters*, 20(2):149–153.
- Kley, T. (2016). Quantile-based spectral analysis in an object-oriented framework and a reference implementation in r: The quantspec package. *Journal of Statistical Software, Articles*, 70(3):1–27.
- Koenker, R. (2005). Quantile regression. *Cambridge University Press*.
- Koenker, R. (2017). Quantile regression: 40 years on. *Annual review of economics*, 9:155–176.
- Koenker, R. and Bassett Jr, G. (1978). Regression quantiles. *Econometrica: journal of the Econometric Society*, pages 33–50.
- Kouretas, G. P., Zarangas, L., et al. (2005). Conditional autoregressive value at risk by regression quantiles: Estimating market risk for major stock markets. Technical report.
- Li, T.-H. (2008). Laplace periodogram for time series analysis. *Journal of the American Statistical Association*, 103(482):757–768.
- Li, T.-H. (2012a). Detection and estimation of hidden periodicity in asymmetric noise by using quantile periodogram. In *Proceedings of the IEEE International Conference on Acoustics, Speech and Signal Processing (ICASSP)*, vol 2, pp. 3969–3972.
- Li, T.-H. (2012b). Quantile periodograms. *Journal of the American Statistical Association*, 107(498):765–776.

- Li, T.-H. (2014). Quantile periodogram and time-dependent variance. *Journal of Time Series Analysis*, 35(4):322–340.
- Li, T.-H. (2023). Quantile-frequency analysis and deep learning for signal classification. *Journal of Nondestructive Evaluation*, 42(2):40.
- Maadooliat, M., Sun, Y., and Chen, T. (2018). Nonparametric collective spectral density estimation with an application to clustering the brain signals. *To appear in Statistics in Medicine*.
- Machado, J. A. and Mata, J. (2005). Counterfactual decomposition of changes in wage distributions using quantile regression. *Journal of applied Econometrics*, 20(4):445–465.
- Martínez-Murcia, F. J., Ortiz, A., Morales-Ortega, R., López, P., Luque, J. L., Castillo-Barnes, D., Segovia, F., Illan, I. A., Ortega, J., Ramirez, J., et al. (2019). Periodogram connectivity of eeg signals for the detection of dyslexia. In *Understanding the Brain Function and Emotions: 8th International Work-Conference on the Interplay Between Natural and Artificial Computation, IWINAC 2019, Almería, Spain, June 3–7, 2019, Proceedings, Part I 8*, pages 350–359. Springer.
- Meziani, A., Medkour, T., and Djouani, K. (2020). Penalised quantile periodogram for spectral estimation. *Journal of Statistical Planning and Inference*, 207:86–98.
- Newey, W. K. and Powell, J. L. (1987). Asymmetric least squares estimation and testing. *Econometrica: Journal of the Econometric Society*, pages 819–847.
- Polat, K. and Güneş, S. (2007). Classification of epileptiform eeg using a hybrid system based on decision tree classifier and fast fourier transform. *Applied Mathematics and Computation*, 187(2):1017–1026.
- Schnabel, S. K. and PHC, E. (2009). Non-crossing smooth expectile curves. In *Proceedings of the 24th International Workshop on Statistical Modelling. Ithaca, NY, USA*, pages 330–36.

- Sharif, A., Bhattacharya, M., Afshan, S., and Shahbaz, M. (2021). Disaggregated renewable energy sources in mitigating co2 emissions: new evidence from the usa using quantile regressions. *Environmental Science and Pollution Research*, 28(41):57582–57601.
- Shumway, R. H. and Stoffer, D. S. (2016). *Time series analysis and its applications: with R examples*. Springer Science & Business Media.
- Waltrup, L. S., Sobotka, F., Kneib, T., and Kauermann, G. (2015). Expectile and quantile regression—david and goliath? *Statistical Modelling*, 15(5):433–456.
- Xu, Q., Chen, L., Jiang, C., and Yu, K. (2020). Mixed data sampling expectile regression with applications to measuring financial risk. *Economic Modelling*, 91:469–486.
- Xu, Q., Ding, X., Jiang, C., Yu, K., and Shi, L. (2021). An elastic-net penalized expectile regression with applications. *Journal of Applied Statistics*, 48(12):2205–2230.
- Yao, Q. and Tong, H. (1996). Asymmetric least squares regression estimation: a nonparametric approach. *Journal of nonparametric statistics*, 6(2-3):273–292.